AGU PUBLICATIONS

Geophysical Research Letters

RESEARCH LETTER

10.1002/2016GL070888

Key Points:
- The strength of the three strongest ENSO events is not separable at 95% confidence level
- The histograms of 1000-member ensemble analysis support that the strength of the three strongest ENSO events is not separable
- The ENSO ranking has to include the SST uncertainty

Correspondence to:
B. Huang,
boyin.huang@noaa.gov

Citation:
Huang, B., M. L'Heureux, Z.-Z. Hu, and H.-M. Zhang (2016), Ranking the strongest ENSO events while incorporating SST uncertainty, *Geophys. Res. Lett.*, *43*, 9165–9172, doi:10.1002/2016GL070888.

Received 26 MAY 2016
Accepted 19 AUG 2016
Accepted article online 23 AUG 2016
Published online 14 SEP 2016

Ranking the strongest ENSO events while incorporating SST uncertainty

Boyin Huang[1], Michelle L'Heureux[2], Zeng-Zhen Hu[2], and Huai-Min Zhang[1]

[1]National Centers for Environmental Information, NOAA, Asheville, North Carolina, USA, [2]Climate Prediction Center, NOAA, College Park, Maryland, USA

Abstract The strength of El Niño–Southern Oscillation (ENSO) is often measured using a single, discrete value of the Niño index. However, this method does not consider the sea surface temperature (SST) uncertainty associated with the observations and data processing. On the basis of the Niño3.4 index and its uncertainty, we find that the strength of the three strongest ENSO events is not separable at 95% confidence level. The monthly peak SST anomalies in the most recent 2015–2016 El Niño is tied with 1997–1998 and 1982–1983 El Niño as the strongest. The three most negative monthly Niño values occur within the 1955–1956, 1973–1974, and 1975–1976 La Niña events, which cannot be discriminated by rank. The histograms of 1000-member ensemble analysis support the conclusion that the strength of the three strongest ENSO events is not separable. These results highlight that the ENSO ranking has to include the SST uncertainty.

1. Introduction

The El Niño–Southern Oscillation (ENSO) is one of the most dominant modes in the Earth climate system. There is tremendous public interest about the strength of ENSO events due to broad societal and economic impacts. In general, the stronger the ENSO event is, the more reliable outlooks of temperature and precipitation anomalies become [e.g., *Kumar et al.*, 2000]. The 2015–2016 El Niño event received considerable attention because of speculation that it could become the strongest El Niño event on record.

ENSO strength is commonly evaluated by sea surface temperatures anomalies (SSTAs) in the tropical Pacific. One popular SSTA index used in the evaluation is the Oceanic Niño Index (ONI), which is defined as 3 month running mean of SSTA in the east central equatorial Pacific Niño3.4 region (5°S–5°N, 120°–170°W) at the NOAA Climate Prediction Center (http://www.cpc.ncep.noaa.gov). To isolate the seasonal-to-interannual variability, the ONI is derived using a climatology of monthly averages spanning multiple, centered, 30 year base periods. The ONI is based on the Extended Reconstructed SST version 4 (ERSSTv4) data set [*Huang et al.*, 2015] and is computed starting in 1950 when the area coverage of situ observations becomes denser (>30%) in the tropical Pacific Ocean. A single value of ONI is presented for each 3 month season and is often used to determine ENSO strength. The advantage of adopting ONI is that it is a simple way to measure ENSO, on the basis of the SSTAs in the east central equatorial Pacific, where the ocean is strongly coupled with the atmosphere [*Barnston et al.*, 1997].

The strength of ENSO can vary depending on region or variable. For example, during the 2000s, a number of El Niño events had their maximum SSTAs in the western or central Pacific, the so-called "Modoki" or "Central Pacific" El Niño event [e.g., *Ashok et al.*, 2007; *Yu and Kim*, 2010; *Hu et al.*, 2012]. As a result, a number of new ENSO indices have been proposed to identify the different flavors of ENSO, such as, using leading Principal Component [e.g., *Ashok et al.*, 2007], rotated Principal Component [e.g., *Takahashi et al.*, 2011], or some combination of the Niño4, Niño3, and Niño1.2 indices [e.g., *Trenberth and Stepaniak*, 2001; *Yeh et al.*, 2009; *Ren and Jin*, 2011]. Moreover, because ENSO is a coupled ocean-atmosphere phenomenon [*Walker*, 1924; *Bjerknes*, 1969; *Wrytki*, 1975] many other indices are used to measure ENSO, such as atmospheric indices based on pressure (e.g., the Southern Oscillation index), winds, and convection anomalies [*L'Heureux et al.*, 2015] and combination indices of the atmosphere and ocean, such as the multivariate ENSO index (MEI) [*Wolter and Timlin*, 2011]. Here we focus on ranking ENSO using SSTAs, though it would be worthwhile to inspect other atmospheric variables and related indices as part of future work.

Not only are there a variety of SST based indices that can be chosen to ascertain ENSO strength but there are also various choices of a SST data set. Among different SST data sets, there are different biases or uncertainties. The uncertainties in an analyzed SST data set can result from errors in in situ observations, choice of analysis methods, and the selection of parameter values that are used to reconstruct or objectively analyze SSTs [*Kennedy et al*., 2011; *Liu et al*., 2015; *Huang et al*., 2016a]. To determine the rank of ENSO events, one needs to test the null hypothesis whether intensity differences are zero among various events. If the null hypothesis cannot be rejected, then it is impossible to rank one ENSO event over another. Such an examination of ENSO strength in the context of SST uncertainty has not been discussed in literature as far as we know, which is the subject of this paper.

2. ERSSTv4 Data Set and Its Uncertainty

2.1. ERSSTv4 Data Set

ERSSTv4 (see *Huang et al*. [2015] for more details) is a monthly 2° × 2° grid analysis that uses in situ SSTs from the International Comprehensive Ocean-Atmosphere Dataset (ICOADS) R2.5 (1854–2007) [*Woodruff et al*., 2011] and the Global Telecommunications System (GTS) receipts (2008 to April 2016) collected by the National Centers for Environmental Prediction (NCEP). ERSSTv4 contains corrections for in situ data biases: (a) ship SST biases associated with different instruments (i.e., buckets and engine room intakes) are corrected using nighttime marine air temperature and (b) buoy SSTs are corrected according to a systematic ship-buoy SST offset of 0.12°C based on observations from 1990 to 2012. The SST reconstruction in ERSSTv4 consists of a low- and high-frequency components. The low-frequency component is constructed from quality-controlled observations by applying a 15 year and 14° × 14° filter. The high-frequency component is constructed from the residual between observation and low-frequency component. The residual is then fitted to a set of localized Empirical Orthogonal Functions. Satellite data are not included because they can introduce a data discontinuity in the 1980s and also their biases are difficult to correct in regions with sparse in situ data for early time periods. SSTAs in this study are derived relative to monthly climatology during 1971–2000. The conventional Niño indices are calculated in Niño4 (5°S–5°N, 160°E–170°W), Niño3.4 (5°S–5°N, 120°–170°W), Niño3 (5°S–5°N, 90°–150°W), and Niño1.2 (0°–10°S, 80°–90°W) regions.

It is important to realize that El Niño and La Niña events defined using a single climatology (e.g., 1971–2000) with fixed thresholds (e.g., +0.5°C) will incorporate longer-term secular or decadal SST trends [e.g., *L'Heureux et al*., 2013]. In section 4, we briefly discuss how the choice of 30 year climatology may affect the magnitude of the SSTA and Niño index values.

2.2. SST Uncertainty Estimation

The currently operational ERSSTv4 is based on optimizing 24 internal parameters, which takes into account errors in in situ observations, data quality control, and instrumental bias adjustments [*Huang et al*., 2016a; for more details]. However, it is important to note that the ERSSTv4 analysis (and other similar SST analyses) can vary when combinations of different, but plausible, parameter values are used to produce an ensemble of ERSSTv4 analyses with large numbers of ensemble members. In fact, a thousand ensemble members are large enough to saturate the uncertainty estimation [*Huang et al*., 2016a]. For each ensemble member, the area-weighted average SSTA is calculated for the conventional Niño indices. Then, the spread of these indices at time t associated with the changes in parameter values is defined as the “parametric uncertainty” ($\sigma(t)_p$) at time t and a grid point or for an index, which is quantified by the standard deviation of the 1000-member ensemble:

$$\sigma(t)_p = \sqrt{\frac{1}{M}\sum_{m=1}^{M}\left(I(t)_m - \overline{I(t)}\right)^2} \tag{1}$$

where $I(t)_m$ is one of the M member indices at time t, $\bar{I}$ is its ensemble average at time t, and M is 1000.

In addition to the parametric uncertainty, an SST reconstruction using a limited set of 130 localized Empirical Orthogonal Functions results in the so-called “reconstruction uncertainty” ($\sigma(t)_r$) in ERSSTv4 [*Huang et al*., 2016a]. The $\sigma(t)_r$ is calculated using the differences between the reconstructed and “perfect” test SSTAs of a 32-member ensemble. The perfect test SSTAs can be from model simulations or other available SST analyses as long as their spatial variability and temporal variability are realistic; thus, the $\sigma(t)_r$ is dependent on the spatial variability of the perfect SSTAs [*Huang et al*., 2016a]. A total of 32 years (1982–2013) data from Daily Optimum Interpolation SST (DOISST) [*Reynolds et al*., 2007] is used as the perfect test SST to estimate $\sigma(t)_r$. Each of the 32 years of SST data is used to generate one member of the ensemble analysis. The $\sigma(t)_r$

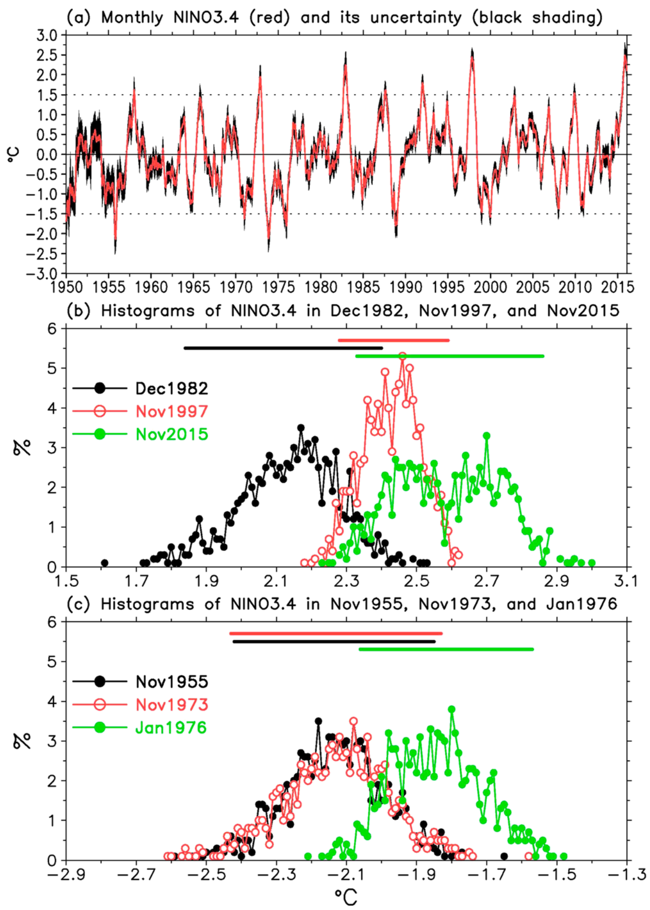

Figure 1. (a) Niño3.4 (solid red line) in ERSSTv4 and its uncertainty (black shading) at the 95% confidence level. (b) Histogram of Niño3.4 in Dec1982 (black), Nov1997 (red), and Nov2015 (green) in 1000-member ensemble analysis, and the horizontal lines indicate their 2.5th–97.5th percentile ranges, respectively. (c) Same as Figure 1b except for Nov1955 (black), Nov1973 (red), and Jan1976 (green). Note that the ensemble averaged Niño3.4 in Figures 1b and 1c is slightly different from Table 1, which represents one realization of the ensemble.

is then defined as the standard deviation of the 32-member ensemble for each individual month from January to December, similar to equation (1).

Since $\sigma(t)_r$ and $\sigma(t)_p$ are nearly uncorrelated [*Huang et al.*, 2015], the overall $\sigma(t)$ is defined as

$$\sigma(t) = \sqrt{\sigma(t)_p^2 + \sigma(t)_r^2} \qquad (2)$$

Huang et al. [2016a] showed that the magnitude of SSTA uncertainty depends largely on (a) the spatial coverage or density of the observations and (b) the domain size for SSTA averaging. The uncertainty of the Niño regions is computed and will be used as a basis to rank ENSO events based on SSTs. The uncertainty changes rapidly from month to month, while the 12 month running average is much smoother. The 12 month running mean uncertainty of the Niño3.4 index is near 0.5°C in the early 1950s and drops to approximately 0.25°C after 1960 (Figure 1a, shading). The parametric uncertainty dominates over the reconstruction uncertainty before 1990 and after 2010, and they are comparable in between. Interestingly, the uncertainty of Niño3.4 noticeably increases after 2010 maybe due to decreased ship observations and the malfunction/vandalism of the Tropical Atmosphere-Ocean (TAO) moorings [*Huang et al*., 2013; *Hu and Kumar*, 2015]. The large uncertainty in the Niño3.4 index motivates us to assess its impacts on the rankings of the strongest El Niño and La Niña events.

3. ENSO Ranking and Impact of SST Data Uncertainty

3.1. Ranking El Niño

The Niño3.4 index (Figure 1a; solid red line) shows that 2015–2016, 1997–1998, and 1982–1983 El Niño events had the three largest monthly averaged values since 1950. The Niño3.4 index peaked at 2.49°C in November 2015, 2.44°C in November 1997, and 2.24°C in December 1982 (Table 1, row 3, columns 2–4). The recent 2015–2016 event had the largest monthly value of Niño3.4. However, for the Niño3 index, the 1997–1998 event had largest peak value (2.59°C in November 2015, 3.15°C in November 1997, and 2.75°C in December 1982; Table 1, row 4, columns 2–4). Using the peak monthly Niño3 index values, one could argue that 1997–1998 event is the strongest. Therefore, the ranking can vary depending on the region, because the location of maximum SSTA changes from event to event. For example, the center of the peak monthly SSTA (2.5°C) during 2015–2016 El Niño is located in the eastern central tropical Pacific (Figure 2c), while it is located farther east for 1997–1998 El Niño (4.0°C) (Figure 2b). The center is located somewhere in between for 1982–1983 El Niño (3.0°C) (Figure 2a).

Table 1. The Monthly Niño4, Niño3.4, Niño3, and Niño1.2 Indices (°C) in Operational ERSSTv4 and Their Corresponding 1.39σ Uncertainties (the Values With ± Sign) Derived From Ensemble Analyses[a]

Indices	Dec1982	Nov1997	Nov2015	Nov1955	Nov1973	Jan1976
Niño4	0.84 ± 0.18 (0.66, 1.02) **Oct1982**	1.00 ± 0.18 (0.82, 1.18)	1.54 ± 0.19 (1.35, 1.73)	−1.50 ± 0.29 (−1.79, −1.21)	−1.61 ± 0.21 (−1.82, −1.40) **Dec1973**	−1.61 ± 0.22 (−1.83, −1.39) **Oct1975**
Niño3.4	2.24 ± 0.24 (2.00, 2.48)	2.44 ± 0.17 (2.27, 2.61)	2.49 ± 0.23 (2.26, 2.72)	−2.13 ± 0.23 (−2.36, −1.90)	−2.12 ± 0.24 (−2.36, −1.88)	−1.80 ± 0.23 (−2.03, −1.57)
Niño3	2.75 ± 0.24 (2.51, 2.99)	3.15 ± 0.20 (2.95, 3.35)	2.59 ± 0.23 (2.36, 2.82)	−2.20 ± 0.33 (−2.53, −1.87) **Oct1955**	−1.68 ± 0.23 (−1.91, −1.45)	−1.76 ± 0.21 (−1.97, −1.56)
Niño1.2	4.01 ± 0.48 (3.53, 4.49) **Jun1983**	3.98 ± 0.26 (3.72, 4.24) **Dec1997**	2.20 ± 0.31 (1.89, 2.51) **Jul2015**	−1.73 ± 0.29 (−2.02, −1.44)	−1.51 ± 0.31 (−1.82, −1.20) **Aug1973**	−2.15 ± 0.28 (−2.43, −1.87) **Nov1975**
ERSSTv3b Niño3.4	2.33 **Jan1983**	2.47	2.77	−2.36	−2.16 **Dec1973**	−1.87
HadISST Niño3.4	2.60 **Jan1983**	2.63	2.74	−1.90	−2.22 **Dec1973**	−1.65
WOISST Niño3.4	2.89 **Jan1983**	2.78	3.06			
DOISST Niño3.4	2.26	2.29	2.90			

[a]These index and uncertainty values are the ones when the Niño3.4 index reaches its monthly maximum/minimum during the El Niño events of 1982–1983, 1997–1998, and 2015–2016 and La Niña events of 1955–1956, 1973–1974, and 1988–1989. The index ranges are listed in parentheses. The peak/trough months are listed in bold when they differ from those of Niño3.4. The Niño index regions are displayed in Figure 2.

While the peak monthly values based on certain SST indices may allow the ranking of one event over another, it is important to test whether these index values are *significantly* different when data uncertainty is considered. Assume that we have two sets of index data; their averaged values are defined as I_1 and I_2; their uncertainties (one standard deviation) are σ_1 and σ_2, respectively. The index ranges in these two data sets at 95% confidence interval in testing the null hypothesis whether the difference of I_1 and I_2 is zero can be expressed by

$$R_1 = (I_1 - 1.39\sigma_1,\ I_1 + 1.39\sigma_1) \tag{3a}$$

$$R_2 = (I_2 - 1.39\sigma_2,\ I_2 + 1.39\sigma_2) \tag{3b}$$

where the number 1.39 is derived from $1.96\times\frac{\sqrt{2}}{2}$. The 1.96 value represents the 95% confidence level, and the $\frac{\sqrt{2}}{2}$ value represents half of the joint uncertainty of $\sqrt{\sigma_1^2+\sigma_2^2}\approx\sqrt{2}\sigma$. If ranges R_1 and R_2 overlap with each other, the null hypothesis is accepted and the indices in those two data sets are considered indistinguishable. Otherwise, the null hypothesis can be rejected and the indices in those two data sets differ significantly.

Table 1 (rows 2–4, columns 2–4) shows that the uncertainties of Niño4, Niño3.4, and Niño3 indices are approximately 0.2°C. The ranges of these Niño index values mostly overlap for the three strongest El Niño events at their maximum monthly values, particularly in Niño3.4 index. Therefore, the null hypothesis that the Niño index strengths are equal can be accepted and distinguishing the relative ranking among the three strongest El Niño events based on the conventional Niño indices is not possible at 95% confidence level. It should be noted, however, that the 2015–2016 El Niño appears to be the strongest if Niño4 and its uncertainty are used to assess El Niño strength (among the selected months in Table 1). In contrast, the 1997–1998 El Niño appears to be the strongest if Niño3 (or Niño1.2) and its uncertainty are used to assess El Niño strength.

To help understand the SST uncertainty derived from the 1000-member ensemble analysis, Figure 1b shows the histograms and their 2.5th–97.5th percentile ranges of the Niño3.4 index for the El Niño events in December 1982, November 1997, and November 2015 when Niño3.4 index reached its maximum. Clearly, the 2.5th–97.5th percentile ranges overlap with each other in these three strongest El Niño events, indicating that these three events are not statistically separable, which is consistent with conclusion based on the uncertainty criterion. Since the ranges of 1982–1983 (1.84°, 2.40°C) and 2015–2016 (2.33°, 2.86°C) in Figure 1b appear to be very close, the significance level is tested when their separation becomes significant. The test shows that their ranges are (1.96°, 2.32°C) and (2.32°, 2.55°C), respectively, at the 10th–90th percentile ranges. This lower significance level makes it less likely that the 2015–2016 El Niño is stronger than the 1982–1983 El Niño.

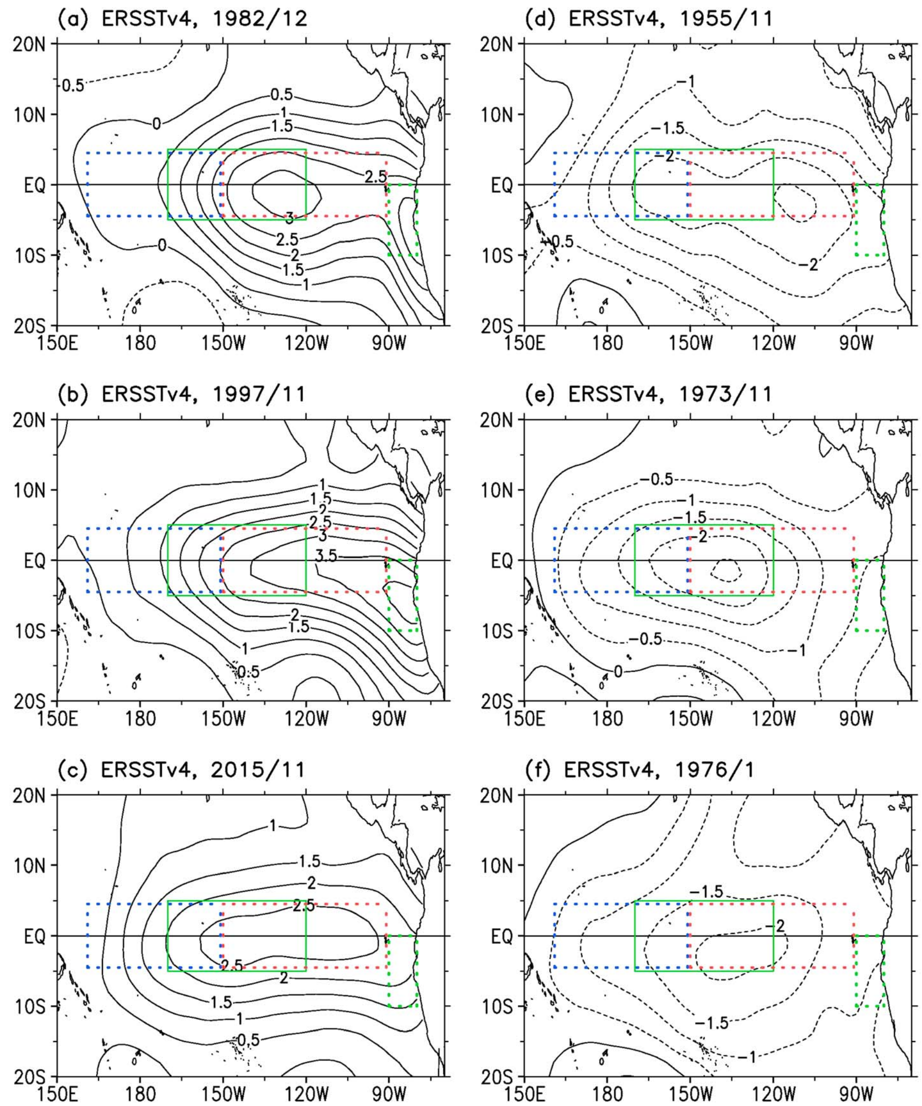

Figure 2. SSTAs in (a) December 1982, (b) November 1997, (c) November 2015, (d) November 1955, (e) November 1973, and (f) January 1976 in ERSSTv4. The Niño4 (5°S–5°N, 160°E–150°W), Niño3 (5°S–5°N, 150°W–90°W), Niño3.4 (170°W–120°W), and Niño1.2 (10°S–0°, 90°W–80°W) areas are indicated by dotted blue, dotted red, solid green, and dotted green boxes.

The uncertainty ranges represented by the 2.5th–97.5th percentile ranges in Figure 1b include the parametric uncertainty only; it does not include the reconstruction uncertainty. Therefore, the actual uncertainty ranges should be wider by including the reconstruction uncertainty as shown in Table 1, which will further support our conclusion that the strength of the 1982–1983 and 2015–2016 El Niño events are not separable. It should also be noted that the ensemble averages (or median) of Niño3.4 in Figures 1b and 1c are not the same as the Niño3.4 in Table 1 that is calculated from the operational ERSSTv4. The operational ERSSTv4 uses the best parametric values according to cross-validation tests [*Huang et al.*, 2015], while the ensemble members use many possible selections for the parameter values. For example, the operational ERSSTv4 uses a ship-buoy offset of 0.12°C, while the ensemble analysis randomly selects the offset of 0.00° or 0.12°C. Therefore, the operational ERSSTv4 is not in the middle of the ensemble members.

3.2. Ranking La Niña

Similarly, sorting by the most negative values in the Niño3.4 index (Figure 1a; solid red line), the 1955–1956, 1973–1974, and 1975–1976 La Niña events are in the top three. The Niño3.4 index values are −2.13°C in November 1955, −2.12°C in November 1973, and −1.80°C in January 1976 (Table 1, row 3, columns 5–7).

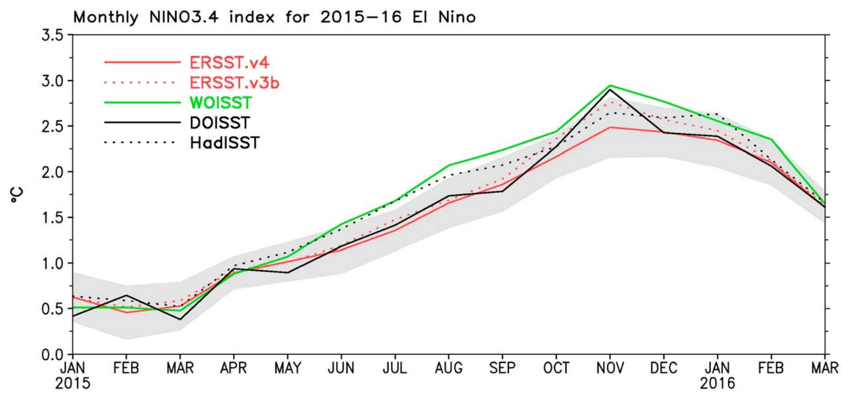

Figure 3. Monthly Niño3.4 from ERSSTv4 (solid red line), ERSSTv3b (dotted red line), WOISST (solid green line), DOISST (solid black line), and HadISST (dotted black line) during 2015–2016 El Niño. The gray shading represents the 1.96σ uncertainty of ERSSTv4 at the 95% confidence level.

Because the uncertainty of the Niño3.4 index is approximately 0.2°C (Table 1, row 3, columns 5–7), there is an overlap in the estimated range of Niño3.4 values. Therefore, the amplitude of the strongest La Niña events cannot be distinguished at the 95% confidence level. Similarly, Niño4, Niño3, and Niño1.2 indices (Table 1, rows 2, 4, and 5, columns 5–7) overlap with each other at the months with minimum monthly value and are also not distinguishable at the 95% confidence level.

The histograms (Figure 1c) of the Niño3.4 index for the La Niña events in November 1955, November 1973, and January 1976 confirm that these three strongest La Niña events are not statistically separable at the 95% confidence level. The 2.5th–97.5th percentile ranges overlap with each other, particularly for 1955–1956 and 1973–1974 events.

3.3. Ranking Using Different SST Products

Some other near-real-time SST data sets are used to check the impact of different SST data sets on the rankings using the peak monthly index values. These data sets are ERSSTv3b from January 1854 to March 2016 [*Smith et al*., 2008], HadISST from January 1850 to March 2016 [*Rayner et al*., 2003], DOISST from January 1982 to March 2016 [*Reynolds et al*., 2007], and Weekly OISST (WOISST) from January 1982 to March 2016 [*Reynolds et al*., 2002]. The ERSSTv3b is an earlier version of ERSSTv4 with differences in the correction of ship SST instrument biases based on nighttime marine air temperature and the ship-buoy offset correction [*Huang et al*., 2015]. The HadISST includes satellite-based SST observations, and the biases of ship SST are corrected using a bucket model [*Kennedy et al*., 2011]. The WOISST and DOISST include the satellite-based SST observations but use different bias correction methods in correcting the satellite-based SST. The ship-buoy offset is corrected in DOISST but not in WOISST, while the ship instrumental biases, albeit small in the modern period, are not corrected in either. Readers can find detailed comparisons of these data sets in *Huang et al*. [2016b]. All data sets are averaged to a monthly 2° × 2° grid box.

The Niño3.4 values from these SST products are generally consistent with that computed from ERSSTv4 (Figure 3), assuming the SST uncertainty in those products is comparable to that in ERSSTv4. The impact on the rankings are also consistent with the uncertainty in ERSSTv4 since 1950 (Table 1, rows 6–9, columns 2–7).

4. Summary and Discussion

We find that the intensity of the three strongest El Niño and La Niña events cannot be statistically distinguished based on the uncertainty derived from ERSSTv4. Specifically, the intensity of 2015–2016 El Niño cannot be distinguished from 1997 to 1998 and 1982 to 1983 El Niño events at 95% confidence level. Among the strongest La Niña events, there is significant overlap in the ranges of uncertainty among 1955–1956, 1973–1974, and 1975–1976. These results based on the uncertainty in the ERSSTv4 analyses are largely consistent with those from other available SST products; thus, it is a challenge to measure the exact intensity or rank of these strongest ENSO events. Understanding the uncertainty in SST products is critical and often neglected in applications related to ENSO. Errors in observations and parameter selections can perturb Niño indices on average by 0.2°–0.3°C, which can certainly impact the ENSO ranking.

It should be emphasized that this study examines only the strongest El Niño and La Niña events using the peak monthly tropical Pacific SSTA. Also, SSTAs are calculated relative to a fixed 1971–2000 monthly mean climatology. When the 30 year climatology is periodically updated, which is a standard practice for national meteorological services (currently most use 1981–2010 as their base line), Niño indices become slightly less positive after 1992 and slightly less negative before 1985 (not shown). Nevertheless, that does not affect the conclusions about the ranking for the strongest three El Niño and La Niña discussed above.

We have focused on the strongest El Niño and La Niña events, which, by definition, are characterized by high-amplitude SSTAs. In reality, ENSO is a coupled ocean-atmosphere phenomenon and its rankings depend on other variables (such as winds, convection, and pressure) in addition to SST and also regions. Here we hope this study provides a benchmark for more comprehensive rankings and a fuller treatment of uncertainty, which should eventually be expanded to other ENSO relevant variables and indices.

Acknowledgments
We appreciated the constructive suggestions and comments from reviewers. Tony Barnston was particularly helpful in providing suggestions. Data set used in generating Table 1 and Figures 1–3 are available at ftp://ftp.ncdc.noaa.gov/pub/data/cmb/ersst/v4/2016.grl.nino.data. The original data can be accessed at ftp.emc.ncep.noaa.gov/cmb/sst/oimonth_v2 for WOISST, ftp://eclipse.ncdc.noaa.gov/pub/OI-daily-v2/NetCDF for DOISST, ftp://ftp.ncdc.noaa.gov/pub/data/cmb/ersst/v3b for ERSSTv3b, ftp://ftp.ncdc.noaa.gov/pub/data/cmb/ersst/v4 for ERSSTv4, and http://www.metoffice.gov.uk/hadobs/hadisst for HadISST. These data sets are archived in NOAA/NCEI except for HadISST. The scientific results and conclusions, as well as any view or opinions expressed herein, are those of the authors and do not necessarily reflect the views of NWS, NOAA, or the Department of Commerce.

References

Ashok, K., S. K. Behera, S. A. Rao, H. Weng, and T. Yamagata (2007), El Niño Modoki and its possible teleconnection, *J. Geophys. Res.*, *112*, C11007, doi:10.1029/2006JC003798.

Barnston, A. G., M. Chelliah, and S. B. Goldenberg (1997), Documentation of a highly ENSO-related SST region in the equatorial Pacific, *Atmos.-Ocean*, *35*, 367–383.

Bjerknes, J. (1969), Atmospheric teleconnections from the equatorial Pacific, *Mon. Weather Rev.*, *97*, 163–172.

Hu, Z.-Z., and A. Kumar (2015), Influence of availability of TAO data on NCEP ocean data assimilation systems along the equatorial Pacific, *J. Geophys. Res. Ocean*, *120*, 5534–5544, doi:10.1002/2015JC010913.

Hu, Z.-Z., A. Kumar, B. Jha, W. Wang, B. Huang, and B. Huang (2012), An analysis of warm pool and cold tongue El Niños: Air-sea coupling processes, global influences, and recent trends, *Clim. Dyn.*, *38*(9-10), 2017–2035, doi:10.1007/s00382-011-1224-9.

Huang, B., M. L'Heureux, J. Lawrimore, C. Liu, V. Banzon, Z.-Z. Hu, and A. Kumar (2013), Why did large differences arise in the sea-surface temperature datasets across the tropical Pacific during 2012?, *J. Atmos. Oceanic Technol.*, *30*, 2944–2953, doi:10.1175/JTECH-D-13-00034.1.

Huang, B., V. F. Banzon, E. Freeman, J. Lawrimore, W. Liu, T. C. Peterson, T. M. Smith, P. W. Thorne, S. D. Woodruff, and H.-M. Zhang (2015), Extended Reconstructed Sea Surface Temperature version 4 (ERSST.v4): Part I. Upgrades and intercomparisons, *J. Clim.*, *28*, 911–930, doi:10.1175/JCLI-D-14-00006.1.

Huang, B., P. W. Thorne, T. M. Smith, W. Liu, J. Lawrimore, V. F. Banzon, H.-M. Zhang, T. C. Peterson, and M. Menne (2016a), Further exploring and quantifying uncertainties for Extended Reconstructed Sea Surface Temperature (ERSST) version 4 (v4), *J. Clim.*, *29*, 3119–3142, doi:10.1175/JCLI-D-15-0430.1.

Huang, B., C. Liu, V. F. Banzon, H.-M. Zhang, T. R. Karl, J. H. Lawrimore, and R. S. Vose (2016b), Assessing the impact of satellite based observations in sea surface temperature trends, *Geophys. Res. Lett.*, *43*, 3431–3437, doi:10.1002/2016GL068757.

Kennedy, J. J., N. A. Rayner, R. O. Smith, D. E. Parker, and M. Saunby (2011), Reassessing biases and other uncertainties in sea surface temperature observations measured in situ since 1850: 1. Measurement and sampling uncertainties, *J. Geophys. Res.*, *116*, D14103, doi:10.1029/2010JD015218.

Kumar, A., A. G. Barnston, P. Peng, M. P. Hoerling, and L. Goddard (2000), Changes in the spread of the variability of the seasonal mean atmospheric states associated with ENSO, *J. Clim.*, *13*, 3139–3151.

L'Heureux, M. L., D. C. Collins, and Z.-Z. Hu (2013), Linear trends in sea surface temperature of the tropical Pacific Ocean and implications for the El Niño–Southern Oscillation, *Clim. Dyn.*, *40*, 1223–1236, doi:10.1007/s00382-012-1331-2.

L'Heureux, M. L., M. K. Tippett, and A. G. Barnston (2015), Characterizing ENSO coupled variability and its impact on North American seasonal precipitation and temperature, *J. Clim.*, *28*, 4231–4245, doi:10.1175/JCLI-D-14-00508.1.

Liu, W., B. Huang, P. Thorne, V. Banzon, H.-M. Zhang, E. Freeman, J. Lawrimore, T. Peterson, T. Smith, and S. Woodruff (2015), Extended Reconstructed Sea Surface Temperature version 4 (ERSST.v4): Part II. Parametric and structural uncertainty estimations, *J. Clim.*, *28*, 931–951, doi:10.1175/JCLI-D-14-00007.1.

Rayner, N. A., D. E. Parker, E. B. Horton, C. K. Folland, L. V. Alexander, D. P. Rowell, E. C. Kent, and A. Kaplan (2003), Global analyses of sea surface temperature, sea ice, and night marine air temperature since the late nineteenth century, *J. Geophys. Res.*, *108*(D14), 4407, doi:10.1029/2002JD002670.

Ren, H.-. L., and F.-. F. Jin (2011), Niño indices for two types of ENSO, *Geophys. Res. Lett.*, *38*, L04704, doi:10.1029/2010GL046031.

Reynolds, R. W., N. A. Rayner, T. M. Smith, D. C. Stokes, and W. Wang (2002), An improved in situ and satellite SST analysis for climate, *J. Clim.*, *15*, 1609–1625, doi:10.1175/1520-0442(2002)015,1609:AIISAS.2.0.CO;2.

Reynolds, R. W., T. M. Smith, C. Liu, D. B. Chelton, K. S. Casey, and M. G. Schlax (2007), Daily high-resolution blended analyses for sea surface temperature, *J. Clim.*, *20*, 5473–5496, doi:10.1175/2007JCLI1824.1.

Smith, T. M., R. W. Reynolds, T. C. Peterson, and J. Lawrimore (2008), Improvements to NOAA's historical merged land-ocean surface temperature analysis (1880–2006), *J. Clim.*, *21*, 2283–2296, doi:10.1175/2007JCLI2100.1.

Takahashi, K., A. Montecinos, K. Goubanova, and B. Dewitte (2011), ENSO regimes: Reinterpreting the canonical and Modoki El Niño, *Geophys. Res. Lett.*, *38*, L10704, doi:10.1029/2011GL047364.

Trenberth, K. E., and D. P. Stepaniak (2001), Indices of El Niño evolution, *J. Clim.*, *14*, 1697–1701, doi:10.1175/1520-0442(2001)014<1697:LIOENO>2.0.CO;2.

Walker, G. T. (1924), Correlation in seasonal variations of weather. IX: A further study of world weather, *Mem. Indian Meteor. Dept.*, *24*, 275–332.

Wolter, K., and M. S. Timlin (2011), El Niño/Southern Oscillation behaviour since 1871 as diagnosed in an extended multivariate ENSO index (MEI.ext), *Int. J. Climatol.*, *31*, 1074–1087, doi:10.1002/joc.2336.

Woodruff, S. D., et al. (2011), ICOADS release 2.5: Extensions and enhancements to the surface 972 marine meteorological archive, *Int. J. Climatol.*, *31*, 951–967, doi:10.1002/joc.2103.

10.1002/2016GL070888

Wrytki, K. (1975), El Niño—The dynamic response of equatorial Pacific Ocean to atmospheric forcing, *J. Phys. Oceanogr.*, *5*, 572–584.
Yeh, S.- W., J.-S. Kug, B. Dewitte, M.-H. Kwon, B. Kirtman, and F.-F. Jin (2009), El Niño in a changing climate, *Nature*, *461*, 511–514, doi:10.1038/nature08316.Yu.
Yu, J.-Y., and S. T. Kim (2010), Identification of central-Pacific and eastern-Pacific types of ENSO in CMIP3 models, *Geophys. Res. Lett.*, *37*, L15705, doi:10.1029/2010GL044082.